

Adiabatic calorimetry and solid state properties above ambient temperature

Fredrik Grønvold

Department of Chemistry, University of Oslo, P.O. Box 1033 Blindern, 0315 Oslo, Norway

Abstract -Some developments in the use of adiabatic-shield calorimeters above ambient temperature are reported, with emphasis on their importance in the study of slow reactions. In addition to the usual demonstration of calorimeter performance in terms of the heat capacity of α -Al₂O₃, fractional enthalpy of fusion determinations as well as heat-capacity measurements on solid/solid transitions ought to be considered as testing experiments. In this connection results on indium and tin are presented. The larger variety of heat-capacity behavior in two-component systems are considered for solid/solid transitions in Ag₂Se, quartz and cristobalite. The usefulness of adiabatic calorimetry in the study of transitions from metastable to stable states is shown for the NiS phases and for wüstite.

INTRODUCTION

Calorimeters with electrically heated shields, which follow the surface temperature of the sample container, offer unique possibilities for accurate determination of thermodynamic properties. They can be operated with intermittent energy inputs, preceded and followed by equilibration periods, or alternatively with a continuous input of energy. In the latter, dynamic mode, the characteristics resemble those of DSC. The energy or enthalpy increments are usually fairly accurate for instantaneous processes, but the corresponding temperatures might be slightly shifted. With step-wise operation the accuracy of enthalpy and temperature determinations can be increased, and even more important, the presence of enthalpy relaxation processes may be discovered and analyzed. When such processes occur above ambient temperature, they might be studied more easily than below, since intermediate, metastable states start transforming after shorter induction periods, and more often go to completion within reasonable time. These advantages of adiabatic calorimetry for reactive substances in the higher temperature region have appealed to me, but also limited the field of study so far to substances which could be made or obtained in sufficiently large quantities (50 - 200 g). Among references to methodic developments in the field, the contributions by West and Westrum (ref. 1), Hemminger and Höhne (ref. 2), and the one by Kagan (ref. 3) might be mentioned. Before looking closer at the adiabatic techniques I should like to make a few comments about drop calorimetry. The method is unsurpassed for enthalpy-increment determinations for substances with negligible intrinsic and extrinsic defect concentrations in the region of interest, like high-purity synthetic sapphire, α -Al₂O₃, except in the vicinity of the melting temperature. When such determinations are carried out with sufficiently small temperature steps, very accurate heat capacities can also be derived. These types of calorimeters are not adiabatic, or impassable, with regard to the sample to be studied, which is quenched in the transfer, with accompanying influences on the observed thermodynamic properties of the substance in question. One way to avoid the quenching effects is to equilibrate the sample as close to ambient temperature as possible, and keep the receiver at a temperature where equilibration is sufficiently fast. Another way to obtain results closer to equilibrium conditions is to use the adiabatic shield technique.

TECHNIQUES

Continuous heating

The continuous-heating technique reached a high level of performance with the work by Moser (ref. 4) at the Physikalisch-Technische Reichsanstalt in Berlin in 1936. The results on nickel, β -brass and quartz, all showing λ -type transitions, are familiar to us through widespread depictions in the literature. Time has shown that the results suffered somewhat from the difficulty in correctly accounting for the heat exchange and dissipation during continuous heating. In addition, the short "equilibration" time during continuous heating is insufficient for characterizing the details of many structural order-disorder processes, even for good thermal conductors. The time element is of marginal importance for electronic processes, like the disappearance of ferromagnetism in nickel. The continuous heating, adiabatic shield technique has been used successfully and been perfected over the years (ref. 1 - 5). Development in the direction of smaller samples (1 - 2 g), inspired through the advances in adiabatic low-temperature calorimetry, has begun. A calorimeter constructed by Mizota et al. (ref. 6) has recently been used by Iishi et al. (ref. 7) in the study of a non-commensurate phase transition.

Step wise heating

The intermittent technique was brought to a high level of perfection by West and Ginnings (ref. 8) about 40 years ago. Its excellent capabilities were demonstrated in work on α -Al₂O₃ up to 800 K, and later on sulfur (ref. 9) up to 700 K. The

calorimeter was remodelled by Oetting and West (ref. 10) and used in heat-capacity determinations on plutonium metal (ref. 11). In addition to the instruments referred to in the above references, I should like to mention the one by Inaba (ref. 12). It is operated in vacuum over the range 70 to 700 K with intermittent heating. Accuracy is better than 0.2 %, and thus comparable with that of the best adiabatic calorimeters hitherto described. The calorimeter cell is of 90Pt10Rh, 30 mm diameter, 45 mm long with 0.2 mm wall thickness. The heater is wound on the outside of the cell and shielded by 0.03 mm silver foil. The heat transfer is $40 \text{ mW}\cdot\text{K}^{-1}$ at 700 K. The wide-range, fully automatic instrument constructed by Zhang (ref. 13), bears some resemblance to the one by Westrum (ref. 1,14). It was tested with $\alpha\text{-Al}_2\text{O}_3$ over the region 80 to 600 K.

The fully automated instrument by Sorai et al. (ref. 15) bridges the low to intermediate temperature region, 13 - 530 K. Calorimeter cells with 30, 10, and 6 cm^3 sample volume were used. The successful operation of the largest cell was shown by the heat-capacity results on benzoic acid (15 - 305 K) and of $\alpha\text{-Al}_2\text{O}_3$ from 60 to 505 K with an inaccuracy 0.25 % over the region 25 to 400 K. Another instrument was developed by Kano (ref. 16) and used in the region 300 to 700 K for studying the heat capacity of solid, liquid and supercooled bismuth, as well as the enthalpy of fusion. On the basis of their previous work (ref. 17), and that by Yamomura et al. (ref. 18), Tan et al. (ref. 19) constructed a calorimeter with 20 cm^3 sample volume for use in the pressure range 0.1 to 15 MPa and temperatures in the range 300 to 600 K. An accuracy of 0.5 % was obtained with water and $\alpha\text{-Al}_2\text{O}_3$ as test substances at 0.1 and 12 MPa pressure.

The first version of the calorimeter which I have been using in the temperature range 300 to 1000 K, was completed in the 1960's (ref. 20). The sample container of 99.99 % Ag is now 29 mm in diameter and 128 mm long, and has a removable bottom of 90Pt10Rh. The wall thickness is 0.4 mm, and the ends are covered by 0.2 mm thick silver shields. Fused silica is the most frequently used sample container material. The vessel has a central well 10 mm in diameter and 105 mm deep, for the 25-ohm resistance thermometer and the 20-ohm heater of 75Pt25Ir. The silver container has 3x4 thermocouple pockets on its outside. Similar pockets are located on the inside of the top, side and bottom shields for the alumina-insulated Pt/90Pt10Rh thermopiles. The double-walled shields contain 90Pt10Rh heating elements for maintaining zero temperature difference between calorimeter and shields, using 3 L&N 9838 Nanovoltmeters as null detectors. Each thermocouple and null detector are floating with respect to the others, and separated by an optocoupler from the recorder, PID controller and zero-switching power amplifier, see Fig. 1. Outside the shields is a heated guard system, also of silver. The whole assembly is placed in a vertical tube furnace with closed bottom. The measuring system and procedures have been completely automated since 1978. Molar heat-capacity values etc. are turned out after completion of each measuring cycle around the clock - sometimes up to a week - with only minor adjustments by the operator. The main measuring instruments are now an HP 3858A multimeter for current and potential measurements, and an ASL 18 AC resistance bridge. The latter makes it possible to determine drift rates more accurately than the earlier-used Mueller bridge by a factor of 10. Thus, slow reactions and relaxation processes can be followed with minimal human effort. Limitations in accuracy stem mainly from undetected local non-adiabaticity, and from light scatter in the zero drift of the calorimeter with time, due to changes in spurious EMF's from changing temperature gradients in thermocouple wires etc.

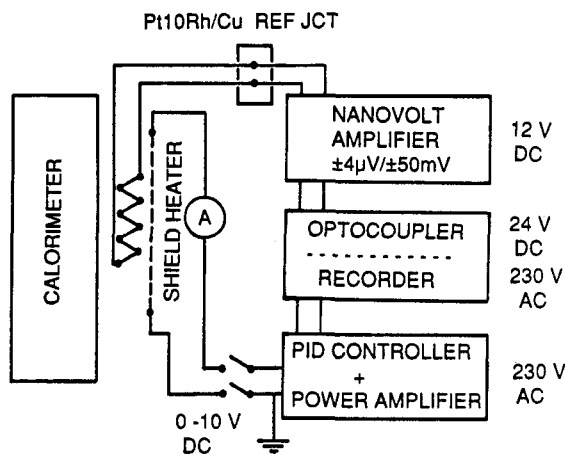


Fig. 1 Shield control system

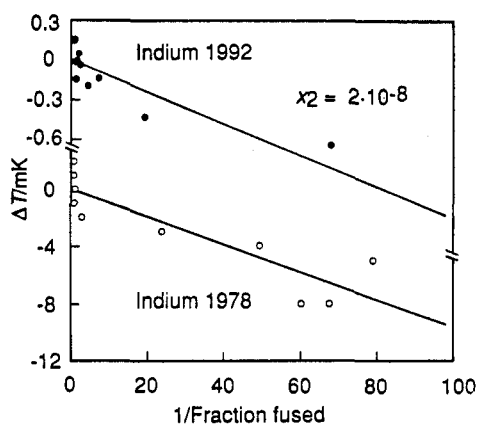


Fig. 2 Fractional fusion of indium

PERFORMANCE TESTS

Synthetic sapphire, $\alpha\text{-Al}_2\text{O}_3$, is a generally used test substance for comparing heat-capacity results with those deduced by Ditmars et al. (ref. 21) on the basis of earlier results. More recent results obtained by adiabatic calorimetry do not seem consistent enough to warrant any change of importance in the range 400 to 900 K.

Few performance tests of the adiabatic calorimeters mentioned have been made on transitions in the pure elements. Oetting and Adams (ref. 11) studied those occurring in plutonium with a modified version of the calorimeter by West and Ginnings (ref. 8), and found a maximum heat capacity of about $15\,000 \text{ J}\cdot\text{K}^{-1}\cdot\text{mol}^{-1}$ for the irreversible α to β transition, which is far

from infinite. For the β to γ and the γ to δ transitions it did not exceed $600 \text{ J}\cdot\text{K}^{-1}\cdot\text{mol}^{-1}$. Similar behavior is characteristic for polymorphism in other elements, like transitions between hexagonal and cubic close packings. Thus, the enthalpy and temperature of melting for very pure metals like indium and tin remain most useful for enthalpy and temperature calibrations. Fractional fusion experiments ought to give heat capacities in the region $10^7 - 10^8 \text{ J}\cdot\text{K}^{-1}\cdot\text{mol}^{-1}$, i.e. a temperature rise of less than 0.1 mK for an energy input 1000 J per mole of substance in the 10 to 90 per cent fusion interval.

Fusion of indium and tin

Results of fractional enthalpy of fusion experiments on a 99.99995 % pure indium sample are shown in Fig. 2 together with results on a less pure sample studied 15 years ago (ref.22). The new sample, which was measured for the Laboratory of the Government Chemist, UK, has a much narrower premelting interval than the earlier sample, consistent with a mole fraction of solid-insoluble/liquid-soluble impurity of the order $2\cdot 10^{-8}$ if the region from 0.4 to 87.8 % fused indium is considered, and $2\cdot 10^{-7}$ if only the region of 13.4 to 88.0 % fusion is taken into account. Over the latter region the temperature rise is $(0.28 \pm 0.08)\text{mK}$, which corresponds to a heat capacity of the order $10^7 \text{ J}\cdot\text{K}^{-1}\cdot\text{mol}^{-1}$. Inside that part of the fusion region the heat capacity might rise to even higher values. The mean result of the five series of enthalpy of fusion determination on a 200 g sample are given in Table 1 together with the unpublished result by Dr. David Ditmars (ref. 23) on NIST SRM (2231) and NPL CRM M16-01, and my earlier determination. They agree reasonably well.

TABLE 1. Enthalpy of fusion determinations on indium and tin

$\Delta_m H_m / (\text{J}\cdot\text{mol}^{-1})$	Purity	Method	Year	Authors	Ref.	$\Delta_m H_m / (\text{J}\cdot\text{mol}^{-1})$	Purity	Method	Year	Authors	Ref.
$M(\text{In}) = 114.818 \text{ g}\cdot\text{mol}^{-1}$						$M(\text{Sn}) = 118.710 \text{ g}\cdot\text{mol}^{-1}$					
3283 ± 7	6N	Adiab.	78	Grønvold	22	7195 ± 7	6N	Adiab.	74	Grønvold	24
$3275 \pm 7^*$	6N	Drop	90	Ditmars	23	7147 ± 22	5N	Drop	89	Ditmars	25
$3283 \pm 7^{**}$	6N	Drop	90	Ditmars	23	7139 ± 18	5N	DSC	92	Callanan	26
3296 ± 9	7N	Adiab.	92	Grønvold	-	7179 ± 15	6N	Adiab.	92	Grønvold	-

* NIST SRM (2231), **NPL CRM M16-01

The results for metallic tin also diverge. Thus, Ditmars result for NIST SRM 2220 was 0.8 % lower than my earlier one. New determinations by adiabatic calorimetry on a different material than I used before are approximately 0.5 % above the ones by Ditmars (ref. 25) and by Callanan (ref. 26). The lower results obtained by drop calorimetry might be real and related to quenching.

In case of a solid insoluble / liquid soluble impurity with mole fraction of the order 10^{-4} it should be possible to recognize an isothermal enthalpy absorption at the eutectic temperature. At temperatures closer to the melting temperature a heat-capacity contribution caused by solution of impurities in the melting solid phase is expected. Tin melts at 505.08 K, and the enthalpy of melting is about $7170 \text{ J}\cdot\text{mol}^{-1}$. With the presence of an ideal solid-insoluble/liquid-soluble impurity with mole fraction $x_{2,\text{tot}} = 1\cdot 10^{-6}$ the fraction fused (F_i) at T_i is (ref.27):

$$F_i = (x_{2,\text{liq}})/(x_{2,\text{tot}}) \approx (x_{2,\text{tot}})RT^2 / [\Delta_m H_m (T_m - T_i)] = 295\cdot 10^{-6} \cdot \text{K}/(T_m - T_i). \quad (1)$$

For $T_m - T_i = \Delta T = 1 \text{ K}$, $F_i = 0.0003$ and for $\Delta T = 17 \text{ mK}$, $F_i = 0.017$. On raising the temperature of a tin sample in the calorimeter about 1 K up to 0.017 K below the fusion temperature the corresponding solution enthalpy increment is $125 \text{ J}\cdot\text{mol}^{-1}$. Similarly, the molar premelting heat capacity observable in adiabatic calorimetry:

$$C_{p,i} \approx (x_{2,\text{tot}})RT^2 / [(T_m - T_i)^2 - (\Delta T/2)^2] \quad (2)$$

should be 2.1 and $9800 \text{ J}\cdot\text{K}^{-1}\cdot\text{mol}^{-1}$ at $T_i = 1 \text{ K}$ and 0.017 K below the fusion temperature, respectively. With the additional presence of solid-soluble/liquid-soluble impurities the melting would occur in a depressed or raised temperature interval, depending upon the impurity distribution between the two phases, and with correspondingly decreased heat capacity.

If the impurity separates out completely from the liquid on quenching in the drop calorimetric experiment, the adiabatic and the drop methods should lead to the same result (except for the strain component due to quenching in the latter), but not so if a small fraction of impurity-rich solution remains incompletely crystallized and is not separated into the components after quenching. Ditmars asserted that the SRM 2220 tin did not show evidence of premelting to within 17 mK from the fusion temperature. In adiabatic calorimetry the pre- and post-melting contributions are routinely included.

TRANSITIONS IN BINARY COMPOUNDS

Some examples of different types of solid/solid transitional behavior are shown in Fig. 3 for an intermediate compound in an X + Y two-component system. The common variant of solid/liquid transitions, where the liquid phase surrounds the solid phase with lower-melting eutectics, has its counterpart in the solid/solid phase eutectoid transition. Here the high-temperature phase (II) form eutectoids on either compositional side of the low-temperature phase (I). If phase (I) has a sensible homogeneity range, various easily depictable heat-capacity behaviors may be encountered (for example a high to infinite heat capacity contribution at the (X) + (I) = (II) eutectoid temperature, followed by a moderate transitional heat capacity

over a wider temperature range). Both processes are kinetically controlled, and the observed heat capacities might show considerable scatter.

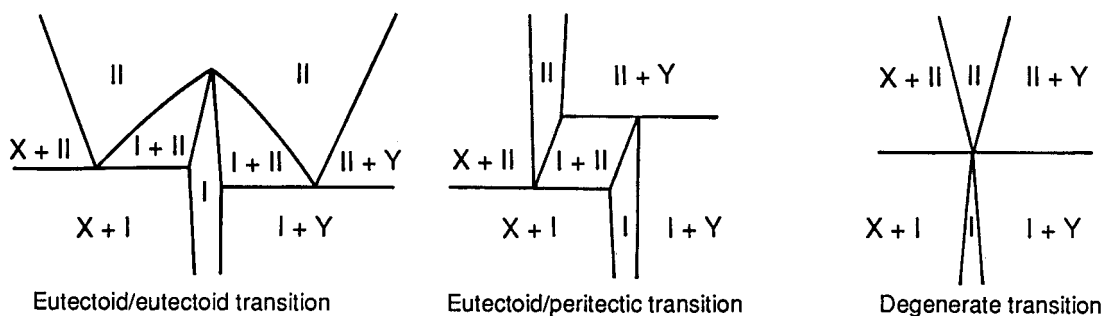


Fig. 3. Sections of temperature - composition diagrams for a binary system.

Another transition variant is the eutectoid/peritectoid one, which is common among solid phases tending towards non-stoichiometry, like some transition metal chalcogenides. Finally one has the case where the two-component phases (I) and (II) are "line" phases with exactly the same stoichiometry. In such cases the low- and the high-temperature phases coexist with identical composition as a degenerate case. Then an intermediate, non-commensurate structural region might exist.

Some of the chalcogenide phases equilibrate relatively fast, and adiabatic calorimetry might be of the right time scale (up to some days equilibration time) for resolving the phase relationships and energies involved. The maximum heat capacity reached varies considerably from system to system. In the case of the transition in stoichiometric FeS at 420 K we found a maximum heat capacity of only $2750 \text{ J}\cdot\text{K}^{-1}\cdot\text{mol}^{-1}$ (ref. 28), while in case of the one in Ni_3S_2 at 834 K it rose to the order $2\cdot 10^5 \text{ J}\cdot\text{K}^{-1}\cdot\text{mol}^{-1}$ (ref.29).

Ag_2Se

The α to β transition in Ag_2Se at about 405 K seemed well suited for investigating the compositional influence on the heat-capacity behavior in binary solid/solid regions, (except that the diffusion rate is somewhat low in the low-temperature phase). The compositional limits of the phases, as determined by coulometric titrations by Valverde (ref. 30), by von Oehsen and Schmalzried (ref. 31), and by Shukla et al. (ref. 32), are combined and redrawn in Fig. 4.

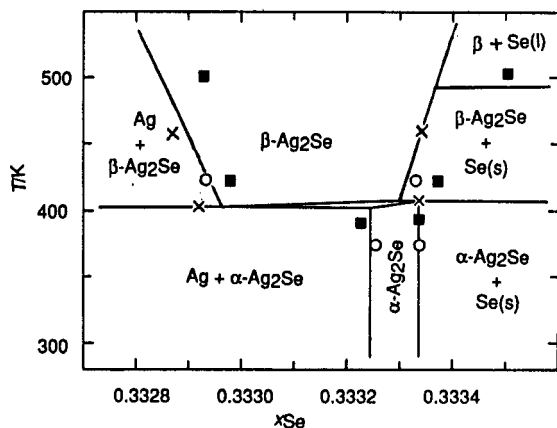


Fig. 4 Section of the Ag - S phase diagram. Phase limits by Valverde, ■; by von Oehsen and Schmalzried, x; and by Shukla et al, o.

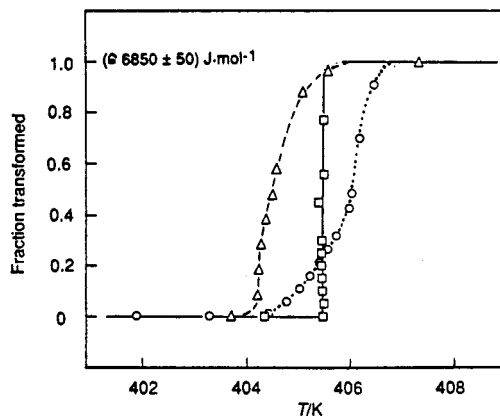


Fig. 5. Fractional enthalpy of transition for $\text{Ag}_{2.005}\text{S}$, Δ ; Ag_2S , o; and $\text{Ag}_2\text{S}_{1.01}$, \square .

Exactly stoichiometric $\alpha\text{-Ag}_2\text{Se}$ should transform peritectoidally into the slightly more silver-rich $\beta\text{-Ag}_{2+x}\text{Se}$ at about 405 K, while a slightly silver-rich $\alpha\text{-Ag}_{2+x}\text{Se}$ should transform in a narrow temperature interval starting at about 403 K. Finally, a suitable mixture of $\alpha\text{-Ag}_2\text{Se}$ and silver ($\text{Ag}_{2.0009}\text{Se} + 0.0026\text{Ag}$) should combine completely at 403 K to give $\beta\text{-Ag}_{2.0035}\text{Se}$. Thus, small compositional variations between samples ought to result in quite different heat-capacity behavior. Another reason for our interest in Ag_2Se is that Shukla et al. (ref. 32) found by DSC that the transitional enthalpy dropped from $7740 \text{ J}\cdot\text{mol}^{-1}$ for $\text{Ag}_{1.999905}\text{Se}$ to $6280 \text{ J}\cdot\text{mol}^{-1}$ for $\text{Ag}_{2.00069}\text{Se}$.

Three high-purity $\text{Ag}_{2\pm x}\text{Se}$ samples are being studied (ref. 33), and some fractional enthalpy of transition results in the transition region are shown in Fig. 5. For $\text{Ag}_2\text{Se}_{1.01}$ the transition occurs almost isothermally at 405.5 K. About 75 % of the transitional enthalpy is acquired within 0.05 K, which corresponds to a transitional heat capacity of $10^5 \text{ J}\cdot\text{K}^{-1}\cdot\text{mol}^{-1}$ with a waiting time of 30 hours. Melting of the excess selenium occurred at about 495 K with an enthalpy of 58 J, which possibly indicates a minute selenium surplus for the $\beta\text{-Ag}_2\text{Se}$ at this temperature ($\Delta_m H_m(\text{Se}) = 6159 \text{ J}\cdot\text{mol}^{-1}$, ref. 34).

The silver-rich sample, $\text{Ag}_{2.005}\text{Se}$, which consists of $\alpha\text{-Ag}_2\text{Se}$ and Ag , suddenly starts to transform at 404.2 K, but the enrichment of silver in the β -phase proceeds slowly. A temperature rise of 0.37 K occurred as result of 6 energy inputs representing about 60 % of the transitional enthalpy, i.e. an average transitional heat capacity of the order $10^4 \text{ J}\cdot\text{K}^{-1}\cdot\text{mol}^{-1}$ during the 15 hour time interval. The transition is about 90 % complete at 405.0 K after 10 additional hours of equilibration, but would presumably have occurred isothermally if the equilibration time had been sufficiently long.

For stoichiometric $\alpha\text{-Ag}_2\text{Se}$ no eutectoid formation reaction is observed, and the transitional heat capacity is of the order $10^3 \text{ J}\cdot\text{K}^{-1}\cdot\text{mol}^{-1}$ from 404.4 to 405.6 K during the 11 h measuring time, indicating a slow compositional change of the high-temperature phase as the temperature goes up. Above 406 K the heat-capacity rise is steeper, possibly for kinetic reasons. Anyway, the heat capacity remains very high above the highest eutectoid temperature. A possible explanation is that the low-temperature phase transforms congruently into the high-temperature phase, just as seems to be the case for Ni_3S_2 . In contrast to the results by Shukla et al.(ref. 32), the presently observed transitional enthalpies differ by less than $100 \text{ J}\cdot\text{mol}^{-1}$, which might indicate that changing kinetic conditions confuses the DSC results. Considerably varying values for the transitional enthalpy have been reported, from $6.95 \text{ kJ}\cdot\text{mol}^{-1}$ by Bellati and Lussana(ref. 35) to the values 9.16 and $10.5 \text{ kJ}\cdot\text{mol}^{-1}$ by Banus(ref. 36), obtained by calorimetry and through use of the Clapeyron equation.

SiO₂

Let me then turn to the α to β transitions in quartz and cristobalite, which we have studied in some detail. The λ -type behavior in quartz was clearly demonstrated in the work by Moser (ref. 4). He made continuous adiabatic measurements in about 10 K steps. The highest heat capacity value was $91 \text{ J}\cdot\text{K}^{-1}\cdot\text{mol}^{-1}$, or far from infinite with present-day technique. Even so Moser claimed the presence of a first-order enthalpy component of $350 \text{ J}\cdot\text{mol}^{-1}$, or about 1/2 of the total, connected with a 0.45 per cent discontinuous volume change. The heat-capacity work by Sinelnikov (ref. 37) did not show any isothermal enthalpy absorption on heating, thus contradicting the presence of the discontinuity. The latter conclusion was strengthened through structural work by Young (ref. 38), which showed that the greatest amplitude of oxygen atom vibrations is in the direction which the oxygen atoms move during the α to β transition. In more recent work the transition is established as non-commensurate over a region of about 1 K (ref.39 - 43). We found no really isothermal enthalpy absorption by adiabatic calorimetry, as the maximum heat capacity was $1700 \text{ J}\cdot\text{K}^{-1}\cdot\text{mol}^{-1}$ only over a 0.02 K interval near 847.30 K (ref. 44). The rise and fall of the curve are very steep and are not easily fit within the common framework for describing the heat-capacity behavior for higher-order transitions (ref. 45,46)

$$\Delta_{\text{trs}}C_p = (A/\alpha) \{ [(T_c - T)/T_c]^{-\alpha} - 1 \} + B$$

where α is the critical exponent, T_c the critical temperature, and A and B empirical constants. The rise is closer to that related to a solid-insoluble/liquid-soluble impurity, see above, or to the incorrect expression for the diverging magnetic heat capacity (ref. 47), $\Delta_{\text{trs}}C_p = A(T_c - T)^{-1/2}$ but the detailed energetics of the transition remain uncertain.

The transition behavior of cristobalite is also puzzling. The α to β cristobalite transition is structurally more drastic than the one in quartz, with its discontinuous volume increase of about 4.5 per cent. According to the heat-capacity study by Smith (ref. 48) and Leadbetter and Smith (ref. 49), the maximum heat capacity is found at 541 K on heating and at 511 K on cooling. The heat capacity rises to the exceptionally moderate value of about $350 \text{ J}\cdot\text{K}^{-1}\cdot\text{mol}^{-1}$, even though the sample was crystallized from vitreous silica at 1690 to 1700 °C for 8 hours. We have measured the heat capacity of a cristobalite sample (ref. 50), obtained by transforming our earlier studied quartz sample at about 1625 °C for 8 hours. Another sample was obtained on loan from Professor Westrum. It was crystallized from quartz at a considerably lower temperature. Heat capacity results in the transition region are shown in Fig. 6. The temperature of the heat-capacity maximum obtained on heating is highest for the Leadbetter/Smith, sample which had been recrystallized at the highest temperature, but surprisingly, the maximum heat capacity is not much higher than for our sample recrystallized 50 K lower. For the sample studied earlier by Westrum (ref. 51) the peak is broad and does not rise above about $140 \text{ J}\cdot\text{K}^{-1}\cdot\text{mol}^{-1}$. The transitional enthalpies are close to the same for all three samples (about $1300 \text{ J}\cdot\text{mol}^{-1}$). The width of the hysteresis temperature interval is reported to increase with the temperature of preparation, while the time for the partial transformation at any temperature is short.

In spite of detailed structural and other studies the reasons for this peculiar behavior still seem in doubt. In the well established, tetragonal structure of α -cristobalite, (ref. 52-54) the two different types of Si - O bond lengths in the SiO_4 tetrahedra are 160.1 and 160.8 pm at ambient temperature, and the tetrahedra share corners with an Si - O - Si angle of 146° . The cubic, structurally improbable arrangement first suggested for β cristobalite by Wyckoff (ref. 55), resulted in a Si - O bond length of 154 pm and Si - O - Si angles of 180° . Nieuwenkamp (ref. 56), saw a solution to this discrepancy in that the oxygen atoms are displaced from their (16-fold) positions normal to the Si - Si axis to six- or twelve-fold positions on a circle with radius of about 45 pm, or perform a hindered rotation on this circle. Thereby satisfactory bond lengths and angles were obtained. The β -cristobalite structure has been studied in more detail by Peacor (ref. 54) and by Wright and Leadbetter (ref. 57). A symmetry analysis of the transition has recently been carried out by Hatch and Ghose (ref. 58). They concluded that the transition involves simultaneous translation and rotation of the SiO_4 tetrahedra coupled in the 110 direction with formation of transformation twins, enantiomorphous twins, and antiphase domains on increasing the temperature.

One hysteresis explanation forwarded by Smith (ref. 48), which seems to have considerable truth, is related to the observation that the transformation of one twin form to another involves much greater atomic rearrangement than the local α to β -

transition. If therefore different domains have different degrees of disorder "locked in" on cooling from the preparation temperature, this disorder is not annealed out at low temperature. Thus, the α to β cristobalite transition seems to equilibrate between metastable states within the time scale of our experiments, and with most of the enthalpy increment related to a local order-disorder process.

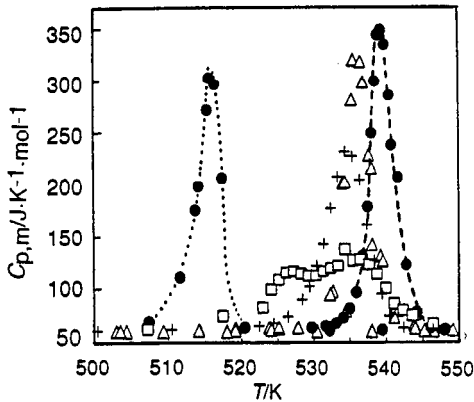


Fig. 6. Heat capacity of cristobalite. $\bullet \bullet$, Smith (cooling); $\bullet - \bullet$, Smith (heating); +, Thompson and Wennemer; Δ , Grønvold and Stølen; \square , Grønvold and Westrum.

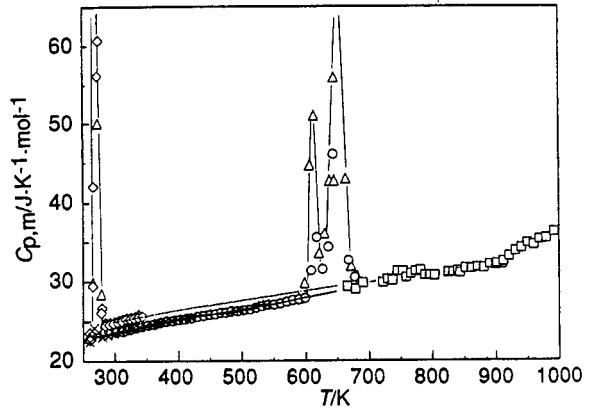


Fig. 7. Heat capacity of NiS. Δ and \diamond , results for NiAs-type phase after quenching the samples from above 660 K; x and o, results for annealed samples (Millerite).

ENTHALPY RELAXATION MEASUREMENTS

In contrast to the transitions considered so far, which are carried out under close to equilibrium conditions, and therefore can be characterized entropy-wise, I will now turn to some that can only be directly characterized enthalpy-wise by adiabatic calorimetry. One such example (ref. 59) is the gradual transition of marcasite to pyrite at about 700 K, which was followed for about 100 h. Pyrite is the stable phase and has the lower entropy of the polymorphs over the whole temperature region.

NiS

For nickel monosulfide 3 different solid phases are of importance: 1) the Millerite phase stable from 0 to 660 K, 2) the semimetallic metastable paramagnetic NiAs-type polymorph ($\mu = 1.7 \mu_B$), existing up to about 270 K, where the volume contracts by 1.7% to 3) the metastable metallic NiAs-type polymorph, which starts transforming to Millerite at about 330 K. Millerite transforms reversibly to the metallic NiAs-type polymorph at about 660 K. This quenchable NiAs-type polymorph can be nickel deficient, which causes a shift in the non-metal to metal transition from 270 K to below 5 K for $Ni_{0.95}S$.

Coey and Brusetti (ref. 60) and Brusetti et al. (ref. 61) measured the heat capacity of quenched NiS and more sulfur-rich samples up to $Ni_{0.95}S$ from 5 to 330 K. Using the Debye model they calculated the entropy difference at 265 K to be $\Delta_{trs}S_m = 3.85 \text{ J}\cdot\text{K}^{-1}\cdot\text{mol}^{-1}$. In addition, the conduction electron entropy increment of the metallic phase was estimated to be $1.70 \text{ J}\cdot\text{K}^{-1}\cdot\text{mol}^{-1}$ at 265 K. The sum agrees well with the observed non-metal to metal transitional entropy, $\Delta_{trs}S_m = (5.32 \pm 0.16) \text{ J}\cdot\text{K}^{-1}\cdot\text{mol}^{-1}$.

We have measured the heat capacity of NiS from 260 K in quenched and annealed states (ref. 62). On heating the quenched NiAs-type phase one first sees the non-metal to metal transition at 270 K, see Fig. 7. The measured entropy increment is

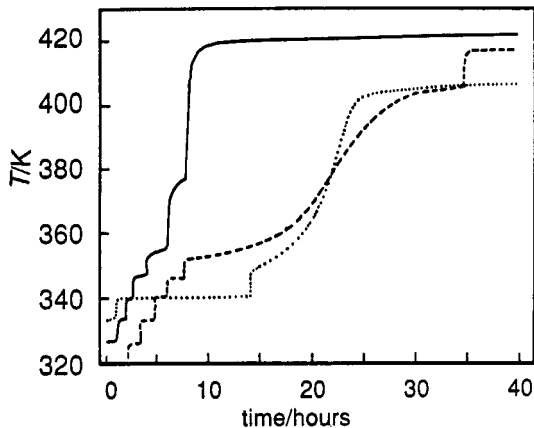


Fig. 8. Transformation of NiAs-type NiS to the Millerite type, Series I to III.

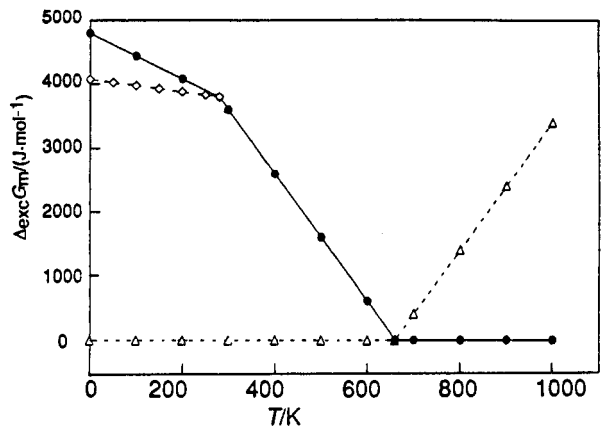


Fig. 9. Excess molar Gibbs energy of formation of NiS phases, relative to the stable one, in the range 0 to 1000 K. \bullet , met. NiAs type, and \diamond , non-met.; Δ , Millerite.

comparable to what Coey and Brusetti (ref. 60) found. Then at about 330 K extra-instrumental drift is observed. Further energy inputs cause the transition to proceed faster. The combined heating and self-heating raise the calorimeter temperature to above 400 K in a matter of 8 to 30 hours, see Fig. 8. The isothermal enthalpy decrement is calculated to be $\Delta_{\text{trs}}H_m(340 \text{ K}) = -5800 \text{ J}\cdot\text{mol}^{-1}$. The heat capacity of the Millerite-type NiS formed rises smoothly with temperature up to 600 K. A small heat-capacity peak at about 610 K is followed by further weak excess enthalpy absorption up to about 660 K where the phase change to the NiAs-type NiS occurs. Thus, with knowledge of the heat capacity of both phases from low temperature, and interpolating it for the metastable one over the range in which it is not easily measured, a complete thermodynamic cycle is obtained, which relates the two phases through their Gibbs energy or enthalpy difference at zero K. See Fig. 9.

Fe_{1-x}O, wüstite

The thermodynamic properties of wüstites, prepared from iron and Fe₂O₃, have been studied recently (ref. 63). Heat capacity measurements on Fe_{0.9379}O show a small maximum at about 190 K (Fig. 10), related to the antiferro- to para-magnetic transition in the oxide. At about 450 K a beginning disproportionation of the metastable wüstite is observed. After complete disproportionation to iron and Fe₃O₄ some measurements were carried out in the 300 to 400 K region, before raising the temperature to about 800 K. The results conform to the values calculated for a mixture of iron and Fe₃O₄. The enthalpy absorption for the decomposition reaction started at about 850 K, and was complete after additional energy inputs and a temperature rise to 892 K during 2 days. In addition to the enthalpy of reaction determination, an evaluation of the thermodynamic properties of wüstite in the metastable region has been carried out. It shows that the molar Gibbs energy decrement of the wüstite phase (expressed by the formula Fe_{1-x}O_x) increases slightly with decreasing x towards stoichiometry. Thus, if iron precipitation is avoided at 500 K, the reaction of wüstite with the mean composition value for two different samples, Fe_{0.932}O = 0.7266 FeO + 0.0684 Fe₃O₄, might proceed with $\Delta_f G_m = -500 \text{ J}\cdot\text{mol}^{-1}$ and $\Delta_f H_m = -2500 \text{ J}\cdot\text{mol}^{-1}$. The exothermic reaction has been studied for a sample with composition Fe_{0.9427}O (ref. 62). It was practically complete after 3 days. X-ray photographs confirm earlier observations (see for example ref. 64), that a mixture of approximately pure FeO (a = 432.8 pm) and Fe₃O₄ (a = 839.4 pm) is obtained. On further heating to about 550 K the final disproportionation of FeO to iron and magnetite starts, and the two reaction enthalpies may therefore be determined separately.

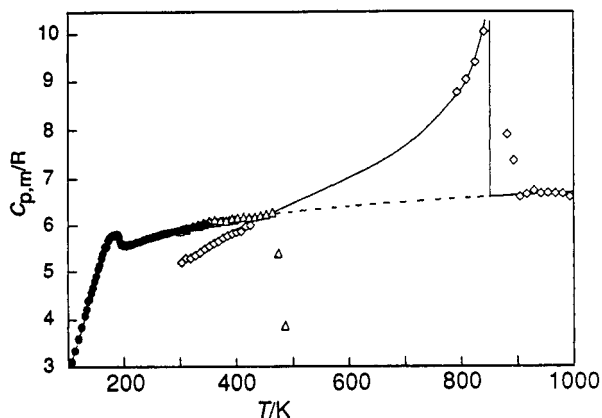


Fig. 10. Molar heat capacity of Fe_{0.9379}O. ●, quenched wüstite 5 - 350 K, Ann Arbor; △, quenched wüstite 300 - 470 K, Oslo; ◇, decomposed wüstite (Fe + Fe₃O₄) 300 to 850 K, and recombined above.

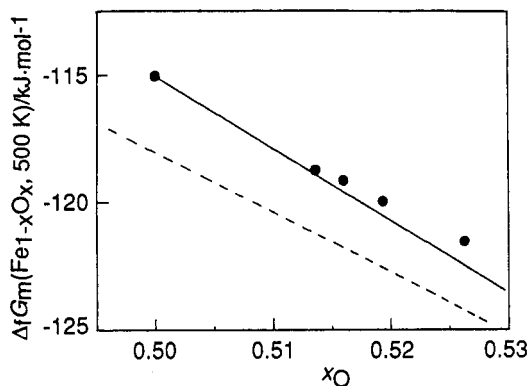


Fig. 11. Estimated molar Gibbs energy of formation for 5 metastable wüstites at 500 K, ●; mixture of FeO and Fe₃O₄, —; mixture of Fe and Fe₃O₄, - -.

These few examples were intended to illustrate some of the capabilities of adiabatic high-temperature calorimetry. A disadvantage at present is the large quantity of sample necessary for accurate work. With the steadily improved accuracy of temperature sensing equipment, and the stability through numerous cycles within the entire measuring range, the sample size might now be reduced without undue loss of accuracy. Platinum sheet resistors and sheet heaters in the shields make size reduction easier, but supposedly not yet adequate for obtaining satisfactory accuracy for most single crystals. Application of pressure and/or magnetic field constitute other important directions of development.

REFERENCES

1. E. D. West and E. F. Westrum, Jr. in *Experimental Thermodynamics, Vol. 1*, J. P. McCullough and D. W. Scott, Eds. Butterworths, London 1968, 333 - 367.
2. W. Hemminger and G. Höhne, *Grundlagen der Kalorimetrie*, Verlag Chemie, Weinheim, 1979.
3. D. N. Kagan in *Compendium of Thermophysical Property Measurement Methods Vol. 1, Survey of Measurement Techniques*, K. D. Maglic, A. Cezairliyan and V. E. Peletsky, Editors, Plenum, New York 1984, 457 - 526.
4. H. Moser *Phys. Z.* 37, 737 - 757 (1936).
5. J. Nörling *Thermochim. Acta* 94, 1 - 15 (1985).
6. T. Mizota, H. Tanaka, Y. Fujii and H. Shima *J. Mineral Soc. Japan* 16, Special Issue 1, 39 - 47 (1983).

7. K. Iishi, T. Mizota, K. Fujino and Y. Furukawa *Phys. Chem. Minerals* 17, 720 - 725 (1991).
8. E. D. West and D. C. Ginnings *J. Res. U.S. Natl. Bur. Standards* 60, 309 - 315 (1958).
9. E. D. West *J. Am. Chem. Soc.* 81, 29 - 37 (1959).
10. F. L. Oetting and E. D. West *J. Chem. Thermodyn.* 14, 107 - 114 (1982).
11. F. D. Oetting and R. O. Adams *J. Chem. Thermodyn.* 15, 537 - 554 (1983).
12. A. Inaba *J. Chem. Thermodyn.* 15, 1137 - 1143 (1983).
13. Z. Zhang, *Sci. Sinica Ser. B* 29, 1239 - 1247 (1986).
14. J. T. S. Andrews, P. A. Norton and E. F. Westrum, Jr. *J. Chem. Thermodyn.* 10, 949 - 958 (1978).
15. M. Sorai, K. Kaji and Y. Kaneko *J. Chem. Thermodyn.* 24, 167 - 180 (1992).
16. K. Kano *J. Phys. E: Sci. Instrum.* 22, 907 - 912 (1989).
17. Z.-C. Tan, L. X. Chou, S. X. Chen, A. X. Yin, Y. Sun, C. J. Ye and X. K. Wang *Sci. Sinica Ser. B* 24, 1014-1026(1983).
18. O. Yamomura, M. Oguni, T. Matsuo, and H. Suga *Bull. Chem. Soc. Japan* 60,1269 -1275 (1987).
19. Tan Zhi-Cheng, Ye Jinchun, Sun Yi, Chen Shuxia and Zhou Lixing *Thermochim. Acta* 183, 29 - 38 (1991).
20. F. Grønvold *Acta Chem. Scand.* 21, 1695 - 1713 (1967).
21. D. Ditmars, S. Ishihara, S. S. Chang, G. Bernstein and E. D. West *J. Res. U.S. Natl. Bur. Std* 87, 159 - 163 (1982).
22. F. Grønvold *J. Thermal Anal.* 13, 419 - 428 (1978).
23. D. A. Ditmars, paper presented at 11. IUPAC Conference on Chemical Thermodynamics, Como, Italy, 1990, p. 537, and personal communication.
24. F. Grønvold *Rev. Chim. Minerale*, 11, 568 - 584 (1974).
25. D. A. Ditmars, *Certificate of Analysis, Standard Reference Material 2220*, NIST, 1989-05-16.
26. J. E. Callanan, K. M. McDermott, R. D. Weir and E. F. Westrum, Jr. *J. Chem. Thermodyn.* 24, 233 - 243 (1992).
27. E. F. Westrum, Jr., G. T. Furukawa and J. P. McCullough in ref. 1, 189 - 191.
28. F. Grønvold and S. Stølen *J. Chem. Thermodyn.* 24, 913 - 936 (1992).
29. S. Stølen, F. Grønvold, E. F. Westrum, Jr. and G. R. Kolonin *J. Chem. Thermodyn.* 23, 77 - 93 (1991).
30. N. Valverde *Z. Phys. Chem. NF* 70, 128 - (1970).
31. U. von Oehsen and H. Schmalzried *Ber. Bunsenges. Phys. Chem.* 85, 7 - 14 (1981).
32. A. K. Shukla, P. Sen and D. D. Sarma *Ber. Bunsenges. Phys. Chem.* 86, 198 - 202 (1982).
33. F. Grønvold, Yu. Semenov and S. Stølen, unpublished results (to appear in *J. Chem. Thermodyn.*?)
34. F. Grønvold *J. Chem. Thermodyn.* 5, 525 - 531 (1973).
35. M. Bellati and S. Lussana *Atti Ist. Veneto, Ser. 6*, 7 1051 - 1059 (1888-89).
36. M. D. Banus *Science* 147, 732 - 733 (1965).
37. N. N. Sinelnikov *Doklady Akad. Nauk SSSR* 92, 369 - 372 (1953).
38. R. A. Young, Final Report, U. S. Air Force, OSR Project A-447.
39. G. Van Tendeloo, J. Van Landuyt and S. Amelinckx *Phys. Stat. Solidi a*30, K11 (1975); see also *ibid.* a33, 723 - 735 (1976).
40. L. Van Goethem, J. Van Landuyt and S. Amelinckx *Phys. Stat. Solidi a*41, 129 - 137 (1977)
41. T. A. Aslanyan and A. P. Levanyuk *Solid State Comm.* 31, 641 (1979); see also *Ferroelectrics* 53, 231 - 234 (1984).
42. G. Dolino, J. P. Bachheimer, B. Berge, C. M. E. Zeyen, G. Van Tendeloo, J. Van Landuyt and S. Amelinckx *J. Physique* 45, 901 - 912 (1984).
43. J. Van Landuyt, G. Van Tendeloo, S. Amelinckx and B. M. Walker *Phys. Rev. B* 31, 2986 - 2992 (1985).
44. F. Grønvold, S. Stølen and S. R. Svendsen *Thermochim. Acta* 139, 225 - 243 (1989).
45. L. P. Kadanoff, W. Götze, D. Hamblen, R. Hecht, E. A. S. Lewis, V. V. Palciauskas, M. Rayl, J. Smith, D. Aspnes and J. Kane *Revs. Mod. Phys.* 39, 395 - 431 (1967).
46. R. F. Wiliinga in *Progress in Low Temperature Physics, Vol. 6 Chap. 8*, C. J. Gorter Editor, North-Holland, Amsterdam 1970.
47. L. Landau and E. Lifshitz, *Statistical Physics*, Clarendon Press, Oxford, 1938, p.212 ff.
48. T. W. Smith, *Thesis*, University of Bristol, UK, March 1972.
49. A. J. Leadbetter and T. W. Smith *Phil. Mag.* 33, 113 - 119 (1976).
50. F. Grønvold and S. Stølen, unpublished results.
51. E. F. Westrum, Jr. unpublished results.
52. W. Nieuwenkamp *Z. Krist.* 92, 82 - 88 (1935).
53. W. A. Dollase *Z. Krist.* 121, 369 - 377 (1965).
54. D. R. Peacor *Z. Krist.* 138, 274 - 298 (1973).
55. R. W. G. Wyckoff *Z. Krist.* 62, 189 - 200 (1925).
56. W. Nieuwenkamp *Z. Krist.* 96, 454 - 458 (1937).
57. A. F. Wright and A. J. Leadbetter *Phil. Mag.* 31, 1391 - 1401 (1975).
58. D. M. Hatch and S. Ghose *Phys. Chem. Minerals* 17, 554 - 562 (1991).
59. F. Grønvold and E. F. Westrum, Jr. *J. Chem. Thermodyn.* 8, 1039 - 1048 (1976).
60. J. M. D. Coey and R. Brusetti *Phys. Rev. Lett.* 32, 1257 (1974).
61. R. Brusetti, J. M. D Coey, G. Czjzch, J. Fink, F. Gompf and H. Schmidt *J. Phys. F: Metal Phys.* 10, 33 -51 (1980).
62. F. Grønvold and S. Stølen, unpublished results.
63. F. Grønvold, S. Stølen, P. Tolmach and E. F. Westrum, Jr. unpublished results.
64. W. A. Fischer and A. Hoffmann *Arch. Eisenhüttenw.* 30, 15 - 22 (1959).